J Therm Anal Calorim (2012) 108:633–645
DOI 10.1007/s10973-011-2155-8

Crystallization of novel poly(ε-caprolactone)-*block*-poly(propylene adipate) copolymers

Stavroula G. Nanaki · George Z. Papageorgiou · Dimitrios N. Bikiaris

MEDICTA2011 Conference Special Chapter

Abstract Poly(ε-caprolactone)-*block*-poly(propylene adipate) (PCL-*block*-PPAd) copolymers were prepared using a combination of polycondensation and ring opening polymerization of ε-CL. ^{1}H-NMR and ^{13}C-NMR spectroscopy showed that the prepared copolymers were block. Also, the copolymer composition was calculated from NMR spectra and was found similar to the feeding ratio. The copolymers formed PCL crystals as was proved by WAXD. The crystallization rates and degree of crystallinity, measured from DSC crystallization experiments, decreased with PPAd content. The equilibrium melting points of PCL were estimated applying the Hoffmann–Weeks method and the observed melting point depression was analyzed using the Nishi–Wang equation which showed that there is some miscibility of the copolymer segments. Isothermal crystallization experiments after self-nucleation were performed to distinguish the nucleation and crystal growth stages during isothermal crystallization. The secondary nucleation theory was then used and the obtained data for crystallization rates, estimated from the inverse of the crystallization half-times, were analyzed. The resulting values for nucleation constant K_g, and also for the surface free energies and work of chain folding, increased with PPAd content due to topological restrictions.

Keywords Biodegradable · Block copolymers · PCL · Propylene adipate · Crystallization

S. G. Nanaki · G. Z. Papageorgiou · D. N. Bikiaris (✉)
Laboratory of Polymer Chemistry and Technology,
Department of Chemistry, Aristotle University of Thessaloniki,
541 24 Thessaloniki, Macedonia, Greece
e-mail: dbic@chem.auth.gr

Introduction

Nowadays, the development of materials that are biodegradable and environmental friendly has gained great attention [1]. Aliphatic polyesters consist a class of important polymers due to their very remarkable characteristics—biodegradability, biocompatibility, and mechanical properties. Among them, polycaprolactone (PCL), polylactides, poly(hydroxy butyrate) (PHB), and poly(butylene succinate) (PBSu) are some of the most extensively used polymers of this class [2, 3]. Aliphatic polyesters became of great interest especially in the field of pharmaceutical technology due to their compatibility with the human organism [4, 5].

PCL is a fully biodegradable semicrystalline polymer, that has a low melting point ($T_m \approx 60$ °C) and a low glass transition temperature ($T_g = -60$ °C). It is non-toxic and compatible with other aliphatic polyesters. PCL of high molecular weight shows similar mechanical properties with low density polyethylene (LDPE) and can easily be formed into blown films and fibers. Unfortunately, its high degree of crystallinity limits the biodegradation rate. In order to increase the biodegradation rate, PCL is copolymerized or blended with polymers that biodegrade faster [6].

In the past synthesis of polyesters of 1,3-propanediol (1,3-PD) was difficult due to the fact that it was not available in sufficient purity and quantity in the market. However, recently new methods have been developed for the production of 1,3-PD with low cost and high quality [7, 8] and this enables polyester production. Thus, only recently, papers dealing with polyesters based on 1,3-PD have been published [9–14].

Block copolymers consist of a most promising class of polymeric materials with application in not only pharmaceutical technology and medicine, but also in nanotechnology and other areas [15–18].

In the present study, novel biodegradable semicrystalline poly(ε-caprolactone)-*block*-poly(propylene adipate) (PCL-*block*-PPAd) copolymers with low propylene adipate content were synthesized following a combination of polycondensation and ring opening polymerization. The materials were characterized and the isothermal crystallization of PCL blocks in the copolymers was investigated.

Experimental

Materials

ε-Caprolactone (ε-CL) (purum 99%) was purchased from Aldrich Chemical Co, dried over CaH_2, and purified by distillation under reduced pressure prior to use. Adipic acid (AA) (purum 99+%) and Tetrabutyl titanate (TBT), used as catalyst, was of analytical grade and it was purchased from Aldrich Chemical Co. 1,3-PD (CAS Number: 504-63-2, Purity: >99.7%) was kindly supplied by Du Pont de Nemours Co. Polyphosphoric acid (PPA) used as heat stabilizer was supplied from Fluka. All other materials and solvents used for the analytical methods were of analytical grade.

Synthesis of the polyesters

Synthesis of aliphatic polyester PPAd was performed following the two-stage melt polycondensation method (esterification and polycondensation) in a glass batch reactor. In brief, the proper amount of adipic acid and 1,3-PD in a molar ratio 1/1.1 and the catalyst TBT (3×10^{-4} mol TBT/mol AA) were charged into the reaction tube of the polycondensation apparatus. The apparatus with the reagents was evacuated several times and filled with nitrogen in order to remove the whole oxygen amount. The reaction mixture was heated at 180 °C under nitrogen atmosphere and stirring at a constant speed (500 rpm) was applied. This first step (esterification) is considered to be completed after the collection of almost all the theoretical amount of H_2O, which was removed from the reaction mixture by distillation and collected in a graduated cylinder. In the second step of polycondensation, PPA was added (5×10^{-4} mol PPA/mol AA). A vacuum (5.0 Pa) was applied slowly over a period time of about 30 min, to avoid excessive foaming and to minimize oligomer sublimation. The temperature was slowly increased to 240 °C, while stirring speed was also increased to 720 rpm. The polycondensation continued for about 2 h, time sufficient to produce polyester with high molecular weight.

The bulk polymerization of ε-CL, in order to synthesize neat PCL, was carried out in 250-cm^3 round-bottomed flask equipped with a mechanical stirrer and a vacuum apparatus. The initiator was added as a solution in toluene at a final concentration of 1×10^{-4} mol per mole of monomer. The polymerization mixture was deaired and purged with dry nitrogen three times. The reaction was carried out for 2 h at 180 °C. Unreacted monomer was removed by distillation by applying a high vacuum (≈5 Pa) slowly, to avoid excessive foaming, over a time period of 15 min. Polymerization was stopped by rapid cooling to room temperature.

PCL-*block*-PPAd copolymers with various CL/PPAd molar ratios, such as 90/10 80/20, and 70/30, were synthesised according to the procedures described by Sereto-udi et al. [6]. In brief, purified PPAd with molecular weight (M_n) 2,500–3,000 g mol^{-1} was added into the same apparatus used for PCL synthesis and the proper amounts of ε-CL monomer were added, as well as TBT (10^{-4} mol TBT/mol ε-CL). Polymerization took place at 180 °C under nitrogen flow and a stirring rate of 500 rpm, while the reaction was completed after 2 h. Unreacted monomer was removed by distillation, applying a high vacuum (≈5 Pa) over a time period of 15 min. Polymerization was stopped by rapid cooling to room temperature.

Polymer characterization

Intrinsic viscosity and molecular weight determinations

Intrinsic viscosity measurements on the isolated polymers were performed using an Ubbelohde viscometer, cap. Oc, at 25 °C. All polymers were dissolved in chloroform in order to obtain solutions of 1% w/v in concentration.

Molecular weight determinations were performed by gel permeation chromatography (GPC) method using a Waters 150C GPC equipped with differential refractometer as detector and three ultrastyragel (103, 104, 105 Å) columns in series. $CHCl_3$ was used as the eluent (1 mL min^{-1}) and measurements were performed at 35 °C. Calibration was performed using polystyrene standards with a narrow molecular weight distribution.

Nuclear magnetic resonance (NMR)

^{1}H-NMR and ^{13}C-NMR spectra of polyesters were obtained using a Bruker spectrometer operating at a frequency of 400 and 75.5 MHz, respectively. Deuterated chloroform ($CDCl_3$) was used as solvent in order to prepare solutions of 5% w/v and the spectra were internally referenced to tetramethylsilane. ^{1}H-NMR spectra were analyzed to determine the compositions of the synthesized copolyesters, while ^{13}C-NMR was also utilized for the determination of the compositions as well as the randomness factor (β) and the average number sequence lengths (L_n) of synthesized copolyesters.

Wide angle X-ray diffraction (WAXD)

X-ray diffraction measurements of the samples were performed by an automated powder diffractometer (PW 1050) with Bragg–Brentano geometry (θ–2θ), using CuK_α radiation ($\lambda = 0.154$ nm) in the angle 2θ range from 5° to 60°.

Thermal analysis

Differential scanning calorimetry (DSC) study was performed using a Perkin-Elmer, Pyris Diamond DSC, calibrated with Indium and Zinc standards. Samples of 5 ± 0.1 mg were used in tests. They were sealed in aluminum pans and heated 50 °C above the melting point at a heating rate 20 °C min^{-1} under nitrogen atmosphere. The samples were held at that temperature for 5 min in order to erase any thermal history. For non-isothermal crystallizations, the sample was cooled by the predetermined cooling rate to −30 °C. Cooling rates varied from 2.5 to 20 °C min^{-1}. The subsequent heating scan was then recorded in order to study the melting behavior of the crystallized sample. The heating rate was 20 °C min^{-1}. If some other rate was used this will be discussed in the specific section. A fresh sample was used in each run. An Intra-cooler 2P cooling device was used to achieve high cooling rates over the temperature region of interest, which was from −75 to 120 °C.

Isothermal crystallization experiments at various temperatures in the range of 30–47.5 °C were performed after self-nucleation of the polyester sample. Self-nucleation measurements were performed analogous to the procedure described by Fillon et al. [19] and Müller et al. [20, 21]. The protocol used is very similar with that described by Müller et al. [20, 21] and can be summarized as follows: (a) heating of the sample and remaining at 120 °C or at the proper temperature for each copolymer for 5 min in order to erase any previous thermal history; (b) subsequent cooling at a rate of 10 °C min^{-1} to 35 °C or at the proper temperature for each copolymer and crystallization for 10 min, which creates a "standard" thermal history; (c) partial melting by heating at 20 °C min^{-1} up to a "self-nucleation temperature," T_s; thermal conditioning at T_s for 1 min. Depending on T_s, the crystalline polyester domains will be completely molten, only self-nucleated or self-nucleated and annealed. If T_s is sufficiently high no self-nuclei or crystal fragments can remain and the sample is then in the so-called Domain I, the complete melting domain. At intermediate T_s values, the sample is almost completely molten but some small crystal fragments or crystal memory effects remain, which can act as self-nuclei during a subsequent cooling from T_s, and the sample is said to be in Domain II, the self-nucleation domain. Finally, if T_s is too low, the crystals will only be partially molten, and the remaining crystals will undergo annealing during the 5 min at T_s, while the molten crystals will be self-nucleated during the later cooling, and the sample is in Domain III, the self-nucleation and annealing domain.; (d) cooling scan from T_s at 200 °C min^{-1} to the crystallization temperature (T_c), where the effects of the previous thermal treatment will be reflected on crystallization; (e) heating scan at 20 °C min^{-1} to 120 °C or to the proper temperature for each copolymer, where the effects of the thermal history will be apparent on the melting signal. Experiments were performed to check that the sample did not crystallize during the cooling to T_c and that a full crystallization exothermic peak was recorded at T_c. In heating scans after isothermal crystallization, the standard heating rate was 20° C/min^{-1}. If some other rate was used this will be discussed in the specific section.

Polarizing light microscopy (PLM)

A polarizing light microscope (Nikon, Optiphot-2) equipped with a Linkam THMS 600 heating stage, a Linkam TP 91 control unit, and also a Jenoptic ProgRes C10Plus camera with the Capture Pro 2.1 software was used for PLM observations.

Results and discussion

Polymer characterization

Synthesis of the copolymers was performed following the procedure which was described in the "Experimental"

Table 1 Intrinsic viscosity [η], Average molecular weight values (M_n, M_w) and polydispersity index (M_w/M_n) of the copolymers

Polymers	[η]/dL g^{-1}	Average M_n/g mol^{-1}	Average M_w/g mol^{-1}	M_w/M_n
PCL	0.53	15,300	47,700	3.12
PPAd/PCL 10/90	0.42	14,600	41,800	2.86
PPAd/PCL 20/80	0.53	16300	40,500	2.48
PPAd/PCL 30/70	0.40	13,200	34,300	2.60
PPAd	0.57	15,700	31,900	2.03

section. The molecular weights of the copolymers were high as one can see in Table 1. This is due to the fact that the hydroxyl end groups contained in PPAd are available to act as initiators for ring opening polymerization of ε-CL monomer [22, 23].

From the ^{1}H-NMR spectrum of PCL, it is possible to identify the characteristic proton peaks of the polymer. The methylene group, *a*, next to the atom of oxygen, gives a characteristic triple peak at 4.02–4.06 ppm. The protons of methylene group *b* absorb at almost the same region giving an eightfold peak at 1.58–1.66 ppm, while the protons of the group *c* gives a multiple peak at 1.32–1.39 ppm. Finally, the protons of the group *d* give a triple peak at 2.26–2.31 ppm. In the ^{1}H-NMR spectrum of PPAd, the shift of the methylene group protons of 1,3-PD, *f*, appears at 1.92–1.98 ppm as a quintuple peak while the protons of the two similar methylene groups, *e*, appear as a characteristic triple peak at 4.12–4.14 ppm (Fig. 1). The protons corresponding to methylene groups of adipic acid, give a single peak at 2.319 ppm owing to methylene groups *g* and a quintuple peak at 1.62–1.65 ppm attributed to methylene groups *h*. The spectra of the copolyesters give characteristic peaks in the same regions without significant shifts.

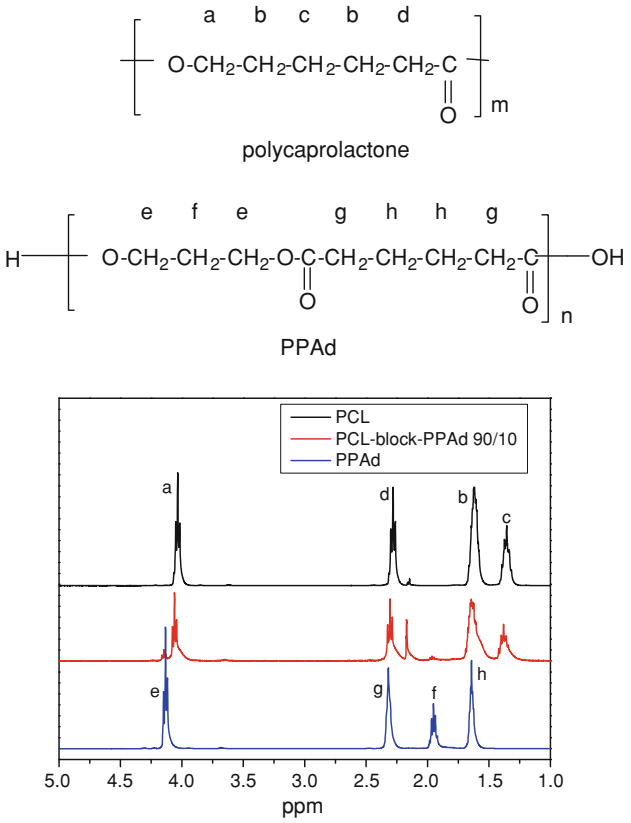

Fig. 1 ^{1}H-NMR spectra of PCL, PPAd, and the PCL-*block*-PPAd 90/10 copolymer

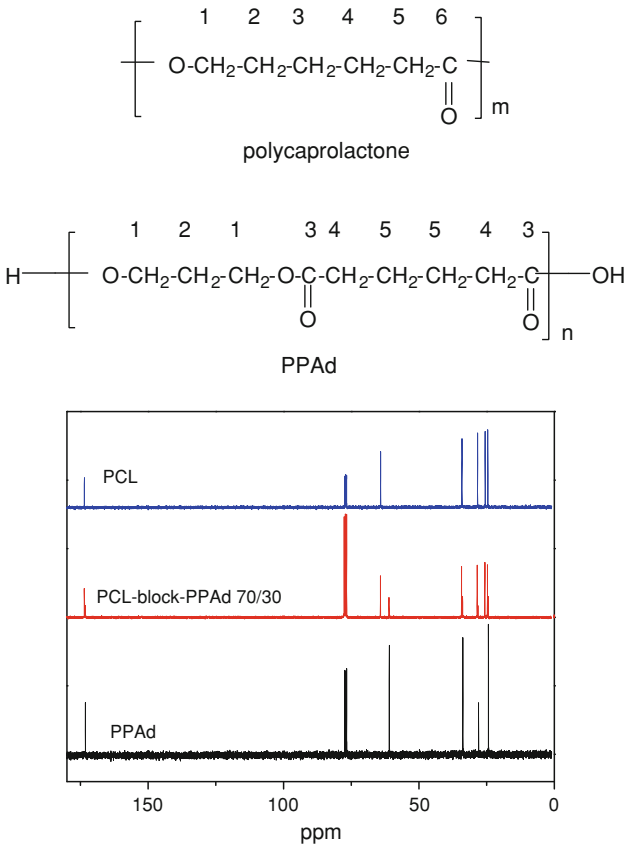

Fig. 2 ^{13}C-NMR spectra of PCL, PPAd, and the PCL-*block*-PPAd 70/30 copolymer

The copolymers with low propylene adipate content were essentially block as was found by ^{13}C-NMR spectra. From ^{13}C-NMR spectra, it is possible to identify the characteristic proton peaks of each polymer. For PCL, the signal at 64.14 ppm corresponds to carbon next to oxygen. The signal at 28.33, 25.23, and 24.57 ppm corresponds to methylene carbons C2, C3, and C4, respectively, while the signal at 34.10 ppm out to carbon next to carbonyl group (C5). Finally, the signal at 173.56 ppm corresponds to the carbonyl carbon (Fig. 2). For PPAd, the signal at 60.92 corresponds to the carbons next to oxygen, while the signals at 27.97 and 24.31 ppm refer to methylene carbons C2 and C5. There are two carbon atoms next to carbonyl groups (C4) and gives a signal at 33.78 ppm. Finally, the signal of the carbonyl carbon (C3) appears at 173.19 ppm. As seen from spectra of their copolymer, PCL-*block*-PPAd 70/30, the signals of both homopolymers are present at the same position.

A closer look at region 173 ppm shows the formation of two new smaller peaks between those ought to neat polymers (Fig. 3). Analogous are the spectra for the other two polyesters. The signals of the copolymer at this region can be identified as follows: (i) the signal at 173.54 ppm owns to carbonyl carbon of PCL moiety (Cl–Cl); (ii) the new

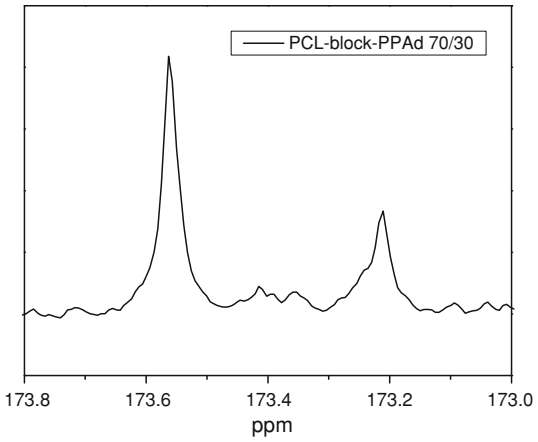

Fig. 3 ^{13}C-NMR spectra of PCL-*block*-PPAd 70/30 copolymer at the region 173–173.8 ppm

signal at 173.39 ppm corresponds to carbonyl carbon of PCL which is bonded to carbonyl carbon of PPAd (Cl–Ad); (iii) the second new signal at 173.33 ppm corresponds to carbonyl carbon of PPAd which is bonded to carbonyl carbon of PCL (Ad–Cl); and (iv) the signal at 173.18 owns to carbonyl carbon of PPAd moiety (Ad–Ad). Integration of these four peaks can be adopted to characterize the chemical microstructures of the synthesized copolymers, i.e., the composition of polyesters, the degree of randomness, and the average number sequence lengths (L_n) [24–26].

The total areas of the four peaks were normalized to one for each copolymer and from normalized areas three possible triad sequences, Cl–Cl–Cl, Cl–Ad–Cl or Ad–Cl–Ad, and Ad–Ad–Ad of copolymers were calculated. The percentage concentration (mol%) of the synthesized copolymers was then calculated using the following equations:

$$\text{PCL } (\%) = P_{\text{PCl}} = P_{(\text{Cl}-\text{Cl}-\text{Cl})} + P_{(\text{Cl}-\text{Ad}-\text{Cl})}/2 \quad (1)$$

$$\text{PPAd } (\%) = P_{\text{PPAd}} = P_{(\text{Ad}-\text{Ad}-\text{Ad})} + P_{(\text{Cl}-\text{Ad}-\text{Cl})}/2 \quad (2)$$

As was found from both NMR spectra, the molar ratios of the copolymers are similar to the initial feeding (Table 2).

The randomness β of the copolymers is calculated by the equation:

$$\beta = P_{(\text{Cl}-\text{Ad}-\text{Cl})}/(2P_{\text{Cl}}P_{\text{Ad}}) \quad (3)$$

When $\beta = 1$ the copolymer takes a random distribution, the value $\beta = 0$ represents blends and when $\beta < 1$ the copolymer take a block distribution. The values calculated for the synthesized copolymers presented in Table 2. As seen, they are ranging from 0.20 to 0.17 indicating that block copolymers have been synthesized.

In order to calculate the average number sequence length of PCL and PPAd to its copolymer, the following equations were used:

$$L_n\text{PCL} = 2P_{\text{PCl}}/P_{(\text{Cl}-\text{Ad}-\text{Cl})} \quad (4)$$

$$L_n\text{PPAd} = 2P_{\text{PPAd}}/P_{(\text{Cl}-\text{Ad}-\text{Cl})} \quad (5)$$

The calculated values are presented in Table 2.

The molecular weight distribution of the prepared polyesters was determined by intrinsic viscosity values as well as by GPC. It can be seen from Table 1 that neat polymers have almost identical molecular weights, 15,300 for PCL and 15,700 g mol^{-1} for PPAd, respectively, while similar are also the molecular weights of the prepared copolymers with small differences.

From the DSC traces of the as received samples, a drop in the melting points for the copolymers with increasing comonomer content (Fig. 4), as well as some reduction in the crystallinity was evidenced for the as received samples, from 65% for neat PCL to about 54% for the PCL-*block*-PPAd) 70/30. Crystallinity values were calculated by dividing the heat of fusion by 136 J g^{-1}, which is the value for the heat of fusion of the fully crystalline PCL [27] and normalizing for the PCL content in the copolymers.

The crystallization rates of the copolymers, under both isothermal and non-isothermal conditions, were found to decrease with increasing comonomer content. The WAXD patterns of the copolymers were studied in order to examine qualitatively the crystallization behavior of the copolymers. The strong crystal diffractions of PCL were expected to appear at angles $2\theta = 21.3°$ for the diffraction of the (110) plane, 22° for the (111) plane, and at 23.8° for the (200) plane [28]. Other weak diffraction peaks also

Table 2 Composition, Randomness factor (β) and the average sequence lengths (L_n) of synthesized copolymers

Polymers	wt%	mol%	mol% ^{1}H-NMR	mol% ^{13}C-NMR[a]	β	L_nCl	L_nPAd
PCL	0/100	0/100	0/100	0/100			
PPAd/PCL 10/90	10/90	6.37/93.63	6.12/93.88	6.35/93.65	0.20	77.27	5.24
PPAd/PCL 20/80	20/80	13.28/86.72	12.97/87.03	13.07/86.93	0.18	43.38	6.52
PPAd/PCL 30/70	30/70	20.80/79.20	23.31/76.69	21.89/78.11	0.17	27.53	7.72
PPAd	100/0	100/0	100/0	100/0			

[a] Estimated from the split carbonyl carbons

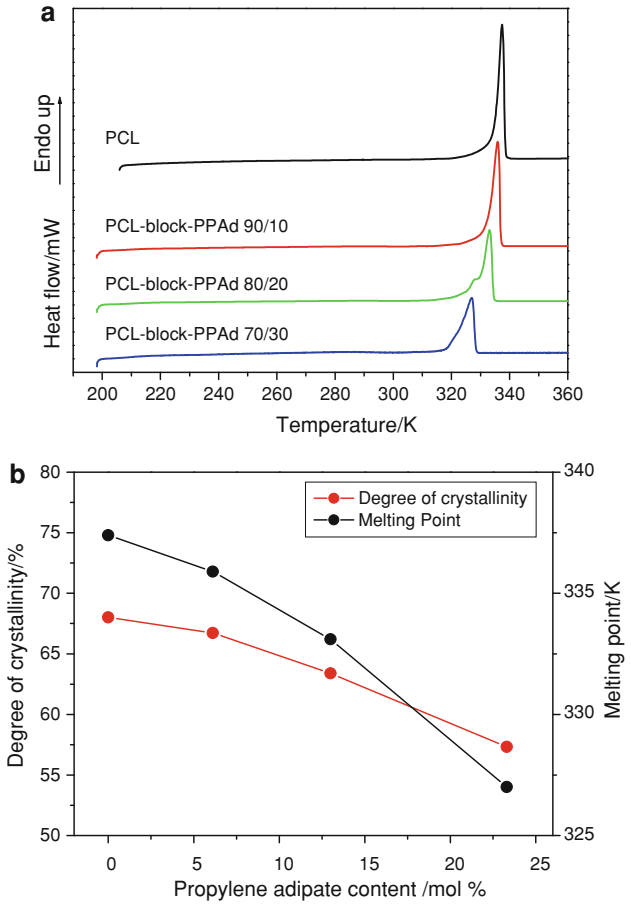

Fig. 4 **a** DSC heating scans of the as received PCL and PCL-*block*-PPAd copolymers at heating rate 20 °C min^{-1} and **b** variation of the degree of crystallinity and the melting point of PCL-*block*-PPAd copolymers with propylene adipate comonomer content

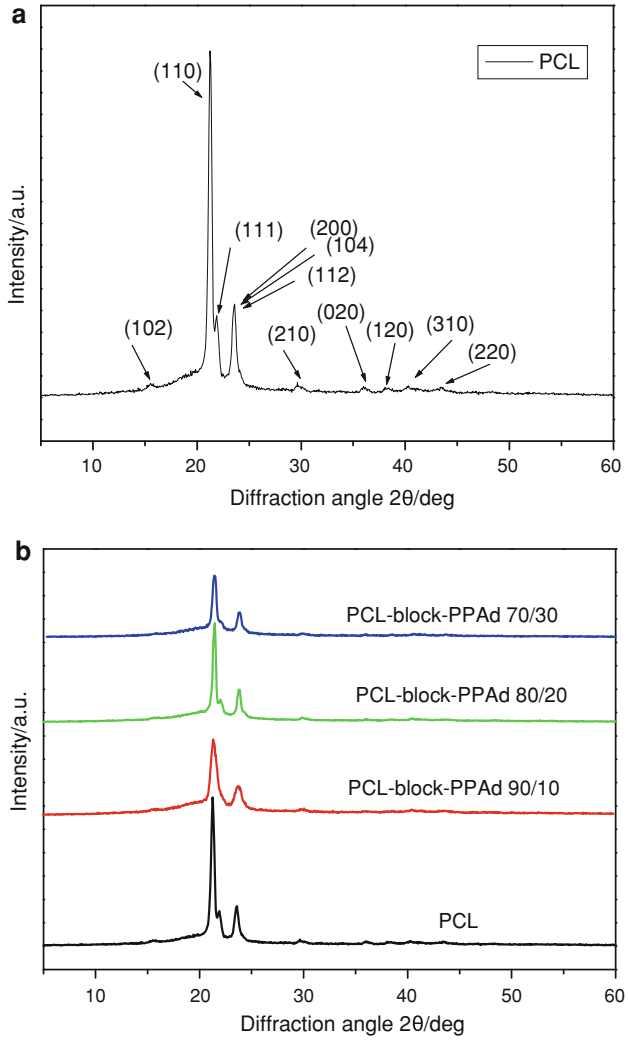

Fig. 5 **a** WAXD patterns of PCL, the diffraction peaks being indexed, **b** WAXD patterns of PCL-*block*-PPAd copolymers

appear in the WAXD pattern of PCL as can be seen in Fig. 5a.

As it is obvious from Fig. 5b, the copolymers gave exclusively PCL crystals. Besides, very slight change in the diffraction angles was observed.

Since observed melting points can be affected by various factors, it is better to use equilibrium melting points for comparison. The most popular method for the estimation of the equilibrium melting point of polymers is that of Hoffman–Weeks, which is favoured by its simplicity and straightforward experimental implementation [29, 30]. According to this procedure, the measured melting temperatures (T_m) of samples isothermally crystallized at various temperatures (T_cs) are plotted against the crystallization temperatures. Linear extrapolation to the line $T_m = T_c$ gives an intercept equal to T_m^0. The associated equation is

$$T_m = \frac{T_c}{2\beta} + T_m^0\left[1 - \frac{1}{2\beta}\right] \quad (6)$$

where T_m^0 is the equilibrium melting temperature, and $\beta = l_c/l^*_c$ is the ratio of lamellar thickness of the mature crystal l_c at the time of melting to the thickness l^*_c of the nucleus. Therefore, β is supposed to be greater or equal to one. The factor 2 is because the thickness of the crystals undergoing melting is about double that of the critical thickness [29, 30].

Before applying the method for the estimation of the equilibrium melting points of PCL-*block*-PPAd copolymers, isothermal crystallizations of PCL and the copolymers were first performed and the subsequent heating scans were recorded to correlate the melting point with the corresponding crystallization temperature (Fig. 6) show the heating scans at a heating rate 20 °C min^{-1} for PCL-*block*-PPAd 90/10 and 80/20, respectively. As can be seen, the ultimate melting peak temperature is directly affected by the crystallization temperature.

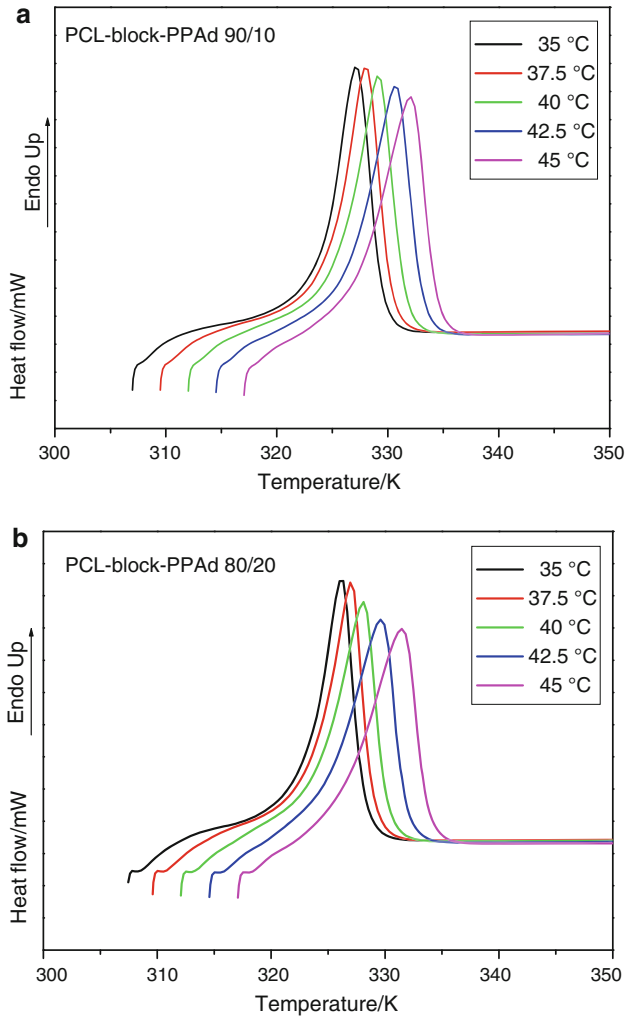

Fig. 6 Subsequent heating scans after isothermal crystallizations at different temperatures: **a** PCL-*block*-PPAd 90/10 and **b** PCL-*block*-PPAd 80/20 copolymer

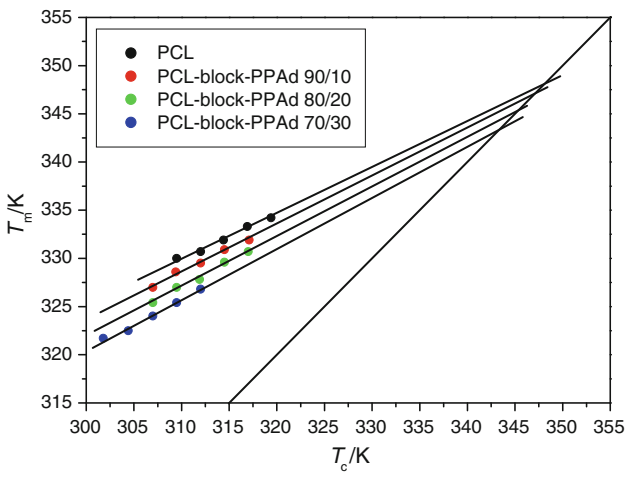

Fig. 7 Hoffman–Weeks plots for neat PCL and the copolymers

In Fig. 7, the Hoffman–Weeks plots for neat PCL as well the copolymers of this study are shown. The T_m^0 values obtained for the copolymers are summarized in Table 3.

To analyze the miscibility of the block segments of the copolymers, the equilibrium melting temperatures were analyzed using the Nishi–Wang equation [31] which in fact is based on the Flory–Huggins theory [32]:

$$\frac{1}{T^0_{m(blend)}} - \frac{1}{T^0_{m(pure)}} = \frac{-R}{\Delta H^0}\frac{V_2}{V_1}\left[\frac{\ln \phi_2}{m_2} + \left(\frac{1}{m_2} - \frac{1}{m_1}\right)\phi_1 + \chi_{12}\phi_1^2\right] \quad (7)$$

In the Nishi–Wang equation [31], the subscripts 1 and 2 refer to the amorphous and the crystalline polymer, respectively. $T^0_{m(pure)}$ and $T^0_{m(blend)}$ denote the equilibrium melting points of the pure crystallizable component and that of the blend, respectively. V is the molar volumes of the repeating units of the polymers, R is the universal gas constant, ΔH^0 is the heat of fusion of the perfectly crystallizable polymer, m is the degree of polymerization, ϕ is the volume fraction of the component in the blend, and χ_{12} is the polymer–polymer interaction parameter. For high molecular weight polymers, both m_1 and m_2 are large and the related terms can be neglected:

$$-\frac{\Delta H^0 V_1}{RV_2}\left(\frac{1}{T^0_{m(blend)}} - \frac{1}{T^0_{m(pure)}}\right) = \chi_{12}\phi_1^2 \quad (8)$$

If χ_{12} is assumed to be independent of the composition, a plot of the left-hand side of Eq. 8 versus ϕ_1^2 should give a straight line passing through the origin. In this study, ΔH^0 for PCL was set equal to 136 J g^{-1} [27]. The molar volumes of the components were calculated using the group contributions [33]. They were found to be $V_1 = 159.5$ cm^3 mol^{-1} of the repeating unit of PPAd, and $V_2 = 104.3$ cm^3 mol^{-1} of the repeating unit of PCL. The experimental data fit a line with a negative slope corresponding to $\chi_{12} = -0.27$, but not passing through the origin (see Fig. 4). The fact that the line does not pass through the origin is usually attributed to a residual entropy effect, which is neglected in the derivation of the equation [34, 35]. A second explanation could be that the interaction parameter χ_{12} is composition dependent. Thus, in the studied block copolymers the result of equilibrium melting point depression shows only some limited miscibility.

Finally, the value of the segregation strength for the prepared copolymers, i.e., the product of the Flory–Huggins parameter times the degree of polymerization was found to be −35.6 suggesting that the polymers form a single phase melt.

Table 3 Temperature, time at the beginning of isothermal crystallization (t_o), time at peak (t_p), heat of crystallization (ΔH), Avrami constant k, composite Avrami constant K and Avrami exponent (n)

Samples	Temperature/°C	t_0/min^{-1}	t_p/min^{-1}	ΔH/J g^{-1}	k/min^{-n}	K/min^{-1}	n
PCL	35.0	0.67	1.03	67.3	6.9343	2.3124	2.31
	37.5	0.70	1.28	66.8	2.1086	1.3664	2.39
	40.0	0.80	1.72	63.5	0.5152	0.7514	2.32
	42.5	0.90	2.90	68.0	0.0865	0.3637	2.42
	45.0	1.00	4.32	66.5	0.0262	0.1866	2.17
	47.5	2.40	9.95	69.2	0.0049	0.0824	2.13
PPAd/PCL 10/90	35.0	0.85	1.75	49.7	0.7925	0.9026	2.27
	37.5	0.90	2.68	56.3	0.1795	0.4645	2.24
	40.0	1.00	4.57	56.9	0.0391	0.2229	2.16
	42.5	1.30	9.10	61.8	0.0081	0.0869	1.97
	45.0	1.85	19.42	68.1	0.0015	0.0290	1.84
PPAd/PCL 20/80	35.0	1.30	3.57	48.0	0.0621	0.3860	2.92
	37.5	1.20	5.20	51.8	0.0105	0.2143	2.96
	40.0	1.40	10.28	51.1	7.47E−4	0.0951	3.06
	42.5	2.60	23.65	52.2	7.25E−5	0.0399	2.96
	45.0	3.20	61.60	43.5	3.19E−6	0.0153	3.03
PPAd/PCL 30/70	30.0	1.00	4.00	46.0	0.0448	0.2814	2.45
	32.5	1.40	10.80	42.3	0.0075	0.0943	2.07
	35.0	1.80	15.50	45.8	0.0011	0.0604	2.43
	37.5	1.15	34.50	43.3	3.68E−5	0.0251	2.77
	40.0	1.36	68.50	35.4	1.403E−5	0.0099	2.42

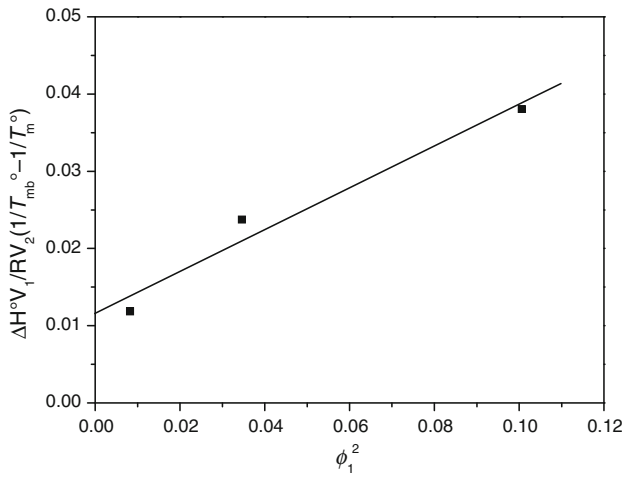

Fig. 8 Plot of $-\frac{\Delta H^0 V_1}{RV_2}\left(\frac{1}{T^0_{m(blend)}}-\frac{1}{T^0_{m(pure)}}\right)$ against ϕ_1^2 according to the Nishi–Wang analysis for melting point depression of PCL in the copolymers

Crystallization kinetics

Isothermal crystallization kinetics

The generated morphology during isothermal crystallization at various temperatures was also studied with the aid of polarized light microscope with hot stage. As can be seen in Figs. 8 and 9, the copolymers formed spherulites. Banded spherulites appeared in most cases of copolymers, with band spacing to increase with temperature. The spherulites became coarse and diffuse with increasing comonomer content and temperature.

Crystallization of polymer melts is usually accompanied by significant heat release, which can be measured by DSC. Based on the assumption that the evolution of crystallinity is linearly proportional to the evolution of heat released during the crystallization, the relative degree of crystallinity, $X(t)$, can be obtained according to the following equation:

$$X(t)=\frac{\int_0^t (\mathrm{d}H_c/\mathrm{d}t)\mathrm{d}t}{\int_0^\infty (\mathrm{d}H_c/\mathrm{d}t)\mathrm{d}t} \tag{9}$$

where $\mathrm{d}H_c$ denotes the measured enthalpy of crystallization during an infinitesimal time interval $\mathrm{d}t$. The limits t and ∞ are used to denote the elapsed time during the course of crystallization and at the end of the crystallization process, respectively.

Isothermal crystallization experiments of the prepared PCL and 90/10, 80/20, and 70/30 copolymers were performed at various temperatures from 35 to 47.5 °C. As the supercooling, i.e., the difference between the melting and crystallization temperature, decreases, the crystallization

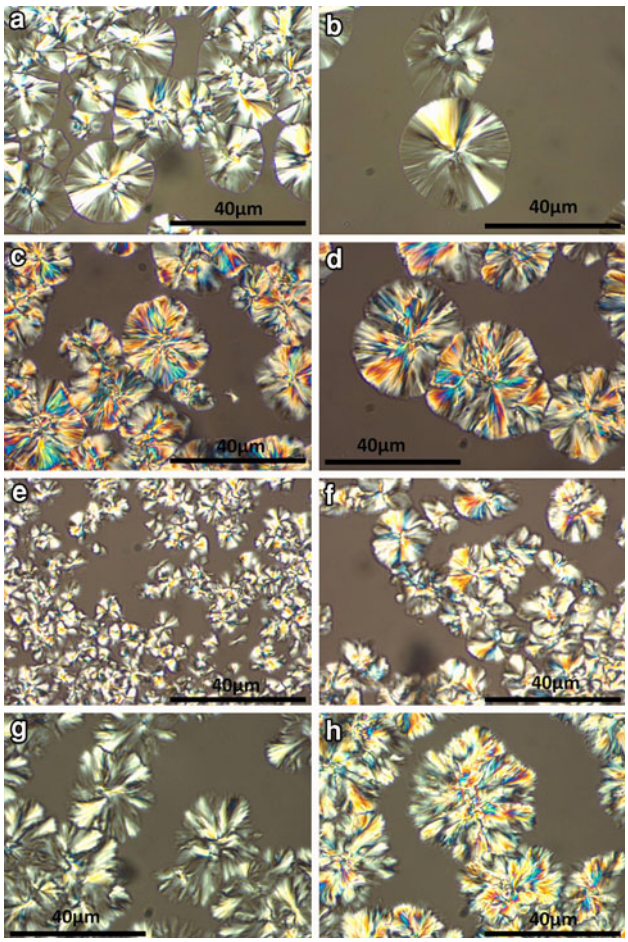

Fig. 9 Spherulitic morphologies generated during isothermal crystallization of: **a**, **b** PCL at 45 °C; **c**, **d** PCL-*block*-PPAd 90/10 at 42.5 °C; **e**, **f** PCL-*block*-PPAd 80/20 at 40 °C; **g**, **h** PCL-*block*-PPAd 70/30 at 40 °C

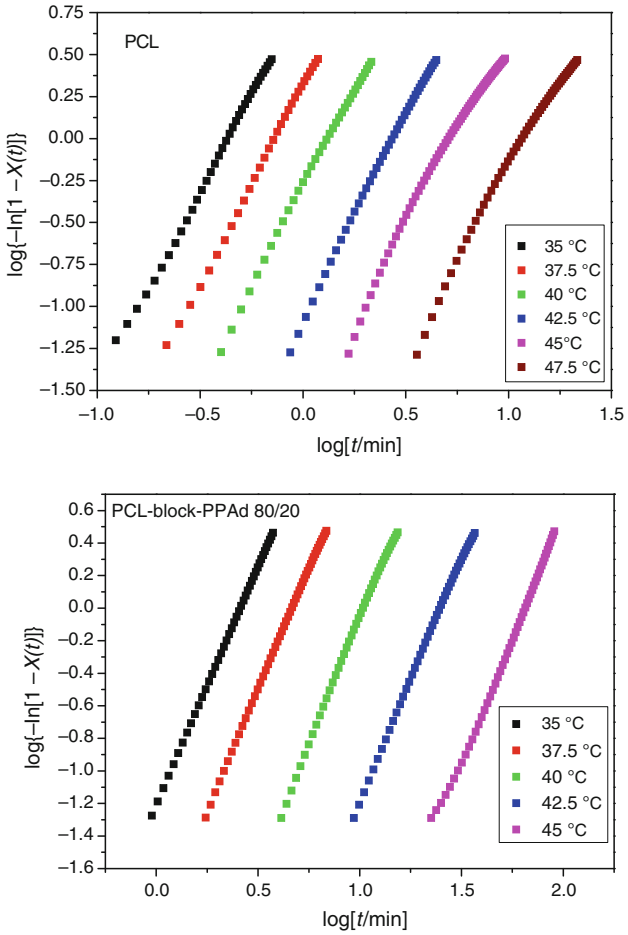

Fig. 10 Avrami plots for neat PCL and the PCL-*block*-PPAd 80/20 copolymer

rate gets slower, and the exothermal peak becomes broader. Thus, the times to reach the peak and to complete crystallization increase.

The crystallization kinetics of the copolymers was investigated using macrokinetic models. For the analysis of the isothermal crystallization, the most common approach is the so-called Avrami method [36–41].

Accordingly, the relative degree of crystallinity, $X(t)$, is related to the crystallization time, t, according to:

$$X(t) = 1 - \exp(-kt^n) \quad \text{or} \quad X(t) = 1 - \exp[-(Kt)^n] \quad (10)$$

where n is the Avrami exponent which is a function of the nucleation process and k is the growth function, which is dependent on nucleation and crystal growth. Since the units of k are a function of n, Eq. 10 can be written in the composite-Avrami form using K instead of k (where $k = K^n$) [42–45].

From the plots of $\log\{-\ln[1 - X(t)]\}$ against $\log t$, $\log k$, and n can be calculated as the intercept and the slope, respectively. Figure 10 shows the Avrami plots for isothermal crystallization of PCL and the 80/20 copolymer.

It is known that the value of n strongly depends on both the mechanism of nucleation and the morphology of crystal growth, and that ideally n would be an integer [36]. The n values found in the case of PCL and copolymers were in principle between 2 and 3 (Table 3). Findings are similar with those for miscible copolymers [39–41].

Secondary nucleation theory

It has been suggested that the kinetic data of isothermal polymer crystallization can be analyzed using the spherulitic growth rate in the context of the Lauritzen–Hoffman secondary nucleation theory [46].

Accordingly, the growth rate G is given as a function of the crystallization temperature, T_c by the following bi-exponential equation 11:

Table 4 Glass transition temperatures (T_g), equilibrium melting points (T_m^o), nucleation parameter K_g, product of surface free energies ($\sigma\sigma_e$), lateral surface free energy (σ), fold surface free energy (σ_e), and work of chain folding (q) values for PCL and PCL blocks in the copolymers

Polymers	T_g/°C	T_m^0/°C	K_g/K^2	$\sigma\sigma_e$/J^2 m^{-4}	σ/J^2 m^{-4}	σ_e/J^2 m^{-2}	q/kJ mol^{-1}
PCL	−66	74	0.83×10^5	6.6×10^{-4}	68.8×10^{-4}	0.0960	21.3
90/10	−65	73.7	1.15×10^5	9.18×10^{-4}	68.8×10^{-4}	0.1335	29.7
80/20	−64	73.1	1.37×10^5	10.9×10^{-4}	68.8×10^{-4}	0.1585	35.2
70/30	−62	70.9	1.55×10^5	12.3×10^{-4}	68.8×10^{-4}	0.1789	39.7

$$G = G_0 \exp\left[-\frac{U^*}{R(T_c - T_\infty)}\right] \exp\left[-\frac{K_g}{T_c(\Delta T)f}\right] \quad (11)$$

where G_0 is the pre-exponential factor, the first exponential term contains the contribution of diffusion process to the growth rate, while the second exponential term is the contribution of the nucleation process; U^* denotes the activation energy which characterizes molecular diffusion across the interfacial boundary between melt and crystals, usually set equal to 1,500 cal mol^{-1} (6,285 J mol^{-1}) and T_∞ is the temperature below which diffusion stops, usually equal to $T_\infty = T_g - 30$ K; K_g is a nucleation constant and ΔT denotes the degree of under-cooling ($\Delta T = T_m^0 - T_c$); f is a correction factor which is close to unity at high temperatures and is given as $f = 2T_c/(T_m^0 + T_c)$; the equilibrium melting temperature, T_m^0 was set equal to 78 °C for PCL, finally the glass transition temperature was assumed equal to −66 °C, while the respective values included in Table 4 were used for the copolymers. The nucleation parameter, K_g, is usually calculated from Eq. 11 using the double-logarithmic transformation (12):

$$\ln(G) + \frac{U^*}{R(T_c - T_\infty)} = \ln(G_0) - \frac{K_g}{T_c(\Delta T)f} \quad (12)$$

Plotting the left-hand side of Eq. 12 with respect to $1/(T_c(\Delta T)f)$, a straight line should appear having a slope equal to K_g.

As was discussed above, the spherulites were diffuse and it was difficult to accurately measure the spherulites diameters in most cases. Instead of using PLM measurements, several authors have treated the isothermal crystallization rate data obtained by DSC, according to the Lauritzen–Hoffman analysis (Eq. 12) [46]. The basic assumption used for the evaluation of G was that the spherulite growth rate is inversely proportional to the crystallization half-time, $G \approx 1/t_{1/2}$ [47]. This approximation although it is purely empirical has been widely used in literature to evaluate the nucleation parameter K_g [47–51]. Müller et al. [20, 21] proposed a self-nucleation procedure for isothermal crystallization to better approximate crystal growth rates, by neglecting nucleation. Then, the resulting $1/t_{1/2}$ values can be used in the Lauritzen–Hoffman analysis. This method was also used in this study.

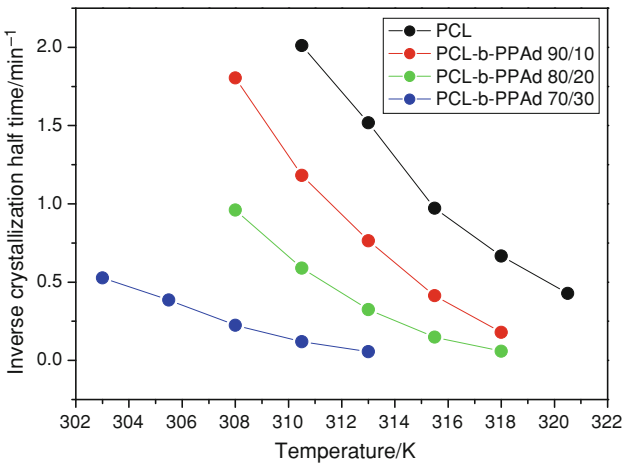

Fig. 11 Variation of the inverse of isothermal crystallization half-times after self-nucleation versus crystallization temperature

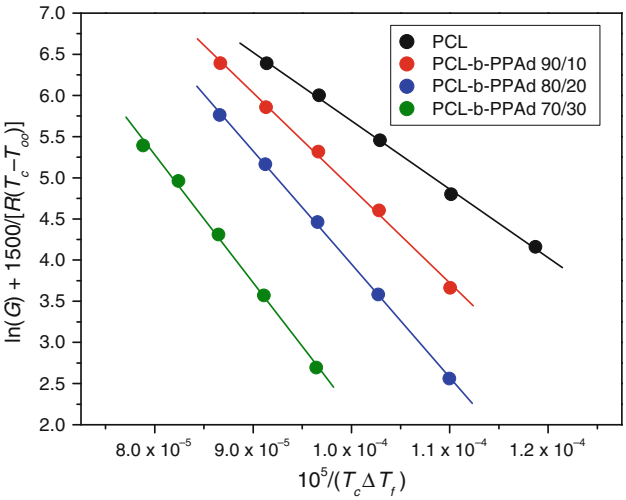

Fig. 12 Lauritzen–Hoffman plots for PCL and PCL-*block*-PPAd copolymers

The relative crystallinity $X(t)$ at time, t, was determined using Eq. 1. From these curves, the half time of crystallization, $t_{1/2}$, was directly determined as the time elapsed from the onset of crystallization to the point where the crystallization is half completed. Half time of crystallization $t_{1/2}$ values increased almost exponentially with the crystallization temperature. In order to compare the

isothermal crystallization rates of the polymeric materials, the reciprocal half-time of crystallization. From the data displayed in Fig. 11, it is apparent that the $t_{1/2}$ values increase almost exponentially as the crystallization temperature is increased, which means that the crystallization rates, denoted by $1/t_{1/2}$, decrease with increasing temperature.

The Lauritzen–Hoffman-type plots for PCL and the copolymers, constructed using the $1/t_{1/2}$ values in the place of G, appear in Fig. 12. The calculated values of K_g for the copolymers are higher than that of neat PCL. Maybe this is associated with topological restrictions experienced by the chains covalently linked to an amorphous and miscible block. These increase as the content of the amorphous block increase.

For a secondary or heterogeneous nucleation, K_g can be calculated from [46]:

$$K_g = \frac{n\sigma\sigma_e b_0 T_m^0}{\Delta h_f \rho_c k_B} \quad (13)$$

where n is a constant equals to 4 for regime I and III and 2 for regime II; σ, σ_e are the side surface (lateral) and fold surface (end) free energies which measure the work required to create a new surface; b_0 is the single layer thickness; $\Delta h_f \rho_c = \Delta H_f$ is the enthalpy of melting per unit volume; and k_B is the Boltzmann constant ($k_B = 1.38\ 10^{-23}$ J K^{-1}). The values used here were $a_0 = 4.5$ Å, $b_0 = 4.1$ Å, and $U^* = 1{,}500$ cal mol^{-1} which correspond to PCL and were also adopted for all materials. The T_m^0 values are included in Table 4. ΔH_f for PCL was taken equal to 136 J g^{-1}, while the unit cell density was taken 1.175 g cm^{-3} for PCL and PCL blocks [27, 52]. It was supposed that regime II holds and thus $n = 2$.

On the other hand, the lateral surface free energy, σ is commonly estimated as [32]:

$$\sigma = \alpha(\Delta h_f)(a_0 b_0)^{0.5} \quad (14)$$

where α was derived empirically to be 0.1 by analogy with the well-known behavior of hydrocarbons. a_0 and b_0 factors are the monomolecular width and layer thickness, respectively. The input data and the results obtained from the secondary nucleation analysis are listed in Table 4.

Finally, the work of chain folding, q, which is most closely correlated with molecular structure, can be calculated from [53]:

$$q = 2a_0 b_0 \sigma_e \quad (15)$$

The results are summarized in Table 4. It seems that all the values for surface free energy or work of chain folding increased for copolymers with the propylene adipate content. This shows effect of PPAd addition on the PCL blocks crystallization.

Conclusions

PCL-*block*-PPAd block copolymers were prepared using a combination of polycondensation and ring opening polymerization of ε-CL. The copolymer composition, as was calculated from NMR spectra, is similar to the feeding ratio of the different monomers in the reactor. The crystal structure of the copolymers was characterized by WAXD. The copolymers formed PCL crystals. The degree of crystallinity of the copolymer samples decreased with increasing comonomer content. The crystallization rates, measured in isothermal experiments using DSC, also decreased with comonomer content. The equilibrium melting points of PCL were estimated following the Hoffmann–Weeks method. Some melting point depression was found. The Nishi–Wang equation was then used to analyze this behavior. The result shows that there is some miscibility of the copolymer segments. The method of Müller et al. was followed to perform isothermal crystallization experiments after self-nucleation, to distinguish between the nucleation and crystal growth stages during isothermal crystallization. The crystallization rates were calculated as the inverse of the crystallization half-times. The secondary nucleation theory was then used and the obtained data for crystallization rates were analyzed. The nucleation constant K_g was found to increase with propylene adipate content, and also the surface free energies and work of chain folding increased, showing inhibition of PCL crystallization.

References

1. Block C, Watzeels N, Rahier H, Van Mele B, Van Assche G. Rheology of nanocomposites: modelling and interpretation of nanofiller influence. J Therm Anal Calorim. 2011;105:731–6.
2. Gan Z, Abe H, Doi Y. Biodegradable poly(ethylene succinate) (PES). 1. Crystal growth kinetics and morphology. Biomacromolecules. 2000;1:704–12.
3. Bikiaris DN, Papageorgiou GZ, Giliopoulos DJ, Stergiou CA. Correlation between chemical and solid state structures and enzymatic hydrolysis in novel biodegradable polyesters. The case of poly(propylene alkanedicarboxylate)s. Macromol Biosci. 2008; 8:728–40.
4. Papadimitriou S, Bikiaris D. Novel self assembled core-shell nanoparticles based on crystalline-amorphous moieties of aliphatic copolyesters for efficient controlled drug release. J Control Release. 2009;138:177–84.
5. Bikiaris DN, Karavelidis V, Karavas E. Novel biodegradable polyesters. Synthesis and application as drug carriers for the preparation of Raloxifene HCl loaded nanoparticles. Molecules. 2009;14:2410–30.
6. Seretoudi G, Bikiaris D, Panayiotou C. Synthesis, characterization and biodegradability of poly(ethylene succinate)/poly(ε-caprolactone) block copolymers. Polymer. 2002;43:5405–15.
7. Hartlep H, Hussmann W, Prayitno N, Meynial-Salles I, Zeng AP. Study of two-stage processes for the microbial production of 1,

3-propanediol from glucose. Appl Microbiol Biotechnol. 2002; 60:60–6.
8. Kim DY, Yim SC, Lee PC, Lee WG, Lee SY, Chang HN. Batch and continuous fermentation of succinic acid from wood hydrolysate by *Mannheimia succiniciproducens* MBEL55E. Enz Microbial Technol. 2004;35:648–53.
9. Wang B, Li CY, Hanzlicek J, Cheng SZD, Geil PH, Grebowicz J, Ho RM. Poly(trimethylene teraphthalate) crystal structure and morphology in different length scales. Polymer. 2001;42:7171–80.
10. Liu Y, Söderqvist-Lindblad M, Ranucci E, Albertsson AC. New segmented poly(ester-urethane)s from renewable resources. J Polym Sci A. 2001;39:630–9.
11. Papageorgiou GZ, Bikiaris DN. Synthesis, cocrystallization and enzymatic degradation of poly(butylene-*co*-propylene succinate) copolymers. Biomacromolecules. 2007;8:2437–49.
12. Papageorgiou GZ, Vassiliou AA, Karavelidis VD, Koumbis A, Bikiaris DN. Novel poly(propylene terephthalate-*co*-succinate) random copolymers Synthesis, solid structure and enzymatic degradation study. Macromolecules. 2008;41:1675–84.
13. Papadimitriou S, Bikiaris DN, Chrissafis K, Paraskevopoulos KM, Mourtas S. Synthesis characterization and thermal degradation mechanism of fast biodegradable PPSu/PCL copolymers. J Polym Sci A. 2007;45:5076–90.
14. Papadimitriou SA, Papageorgiou GZ, Bikiaris D. Crystallization and enzymatic degradation of novel poly(ε-caprolactone-*co*-propylene succinate) copolymers. Eur Polym J. 2008;44:2356–66.
15. Kissel T, Li Y, Unger F. ABA-triblock copolymers from biodegradable polyester A-blocks and hydrophilic poly(ethylene oxide) B-blocks as a candidate for in situ forming hydrogel delivery systems for proteins. Adv Drug Deliv Rev. 2002;54:39–99.
16. Castillo RV, Müller AJ. Crystallization and morphology of biodegradable or biostable single and double crystalline block copolymers. Prog Polym Sci. 2009;34(6):516–60.
17. Hamley IW. Ordering in thin films of block copolymers: Fundamentals to potential applications. Prog Polym Sci. 2009;34: 1161–210.
18. Müller AJ, Balsamo V, Arnal ML. Nucleation and crystallization in diblock and triblock copolymers. Adv Polym Sci. 2005;190: 1–63.
19. Fillon B, Wittmann JC, Lotz B, Thierry A. Self-nucleation and recrystallization of isotactic polypropylene (A phase) investigated by differential scanning calorimetry. J Polym Sci B. 1993;31: 1383–93.
20. Müller AJ, Albuerne J, Marquez L, Raquez JM, Degée P, Dubois P, Hobbs J, Hamley IW. Self-nucleation and crystallization kinetics of double crystalline poly(*p*-dioxanone)-*b*-poly(ε-caprolactone) diblock copolymers. Faraday Discuss. 2005;128:231–52.
21. Boschetti-de-Fierro A, Lorenzo AT, Müller AJ, Schmalz H, Abetz V. Crystallization kinetics of PEO and PE in different triblock terpolymers: effect of microdomain geometry and confinement. Macromol Chem Phys. 2008;209:476–87.
22. Endo M, Aida T, Onoue S. "Immortal" polymerization of ε-caprolactone initiated by aluminum porphyrin in the presence of alcohol. Macromolecules. 1987;20:2982–8.
23. Kricheldorff HR, Berl M, Scharnagl N. Poly(lactones). 9. Polymerization mechanism of metal alkoxide initiated polymerizations of lactide and various lactones. Macromolecules. 1988;21: 286–93.
24. Chen CH, Peng JS, Chen M, Lu HY, Tsai CJ, Yang CS. Synthesis and characterization of poly(butylene succinate) and its copolyesters containing minor amounts of propylene succinate. Colloid Polym Sci. 2010;7:731–8.
25. Chen CH, Lu HY, Chen M, Peng JS, Tsai CJ, Yang CS. Synthesis and characterization of poly(ethylene succinate) and its copolyesters containing minor amounts of butylene succinate. J Appl Polym Sci. 2009;111:1433–9.
26. Ko CY, Chen M, Wang HC, Tseng IM. Sequence distribution, crystallization and melting behavior of poly(ethylene terephthalate-*co*-trimethylene terephthalate) copolyesters. Polymer. 2005;46:8752–62.
27. Barham PJ, Keller A, Otun EL, Holmes PA. Crystallization and morphology of a bacterial thermoplastic: poly-3-hydroxybutyrate. J Mater Sci. 1984;19:2781–94.
28. Chatani Y, Okita Y, Tadoloro H, Yamashita Y. Structural studies of polyesters. III. Crystal structure of poly-ε-caprolactone. Polym J. 1970;1:555–62.
29. Hoffman JD, Weeks JJ. Melting process and equilibrium melting temperature of polychlorotrifluoroethylene. Res Natl Bur Stand. 1962;66A:13–8.
30. Hoffman JD, Davis GT, Lauritzen JI Jr. In: Hannay B. N, editor. Treatise on solid state chemistry, vol. 3, Chap 7. New York: Plenum Press; 1976.
31. Nishi T, Wang TT. Melting point depression and kinetic effects of cooling on crystallization in poly(vinylidene fluoride)-poly (methyl methacrylate) mixtures. Macromolecules. 1975;8:909–15.
32. Flory PJ. Principles of polymer chemistry. Ithaca: Cornell University Press; 1953.
33. Van Krevelen DW, Hopfytzer PJ. Properties of polymers, correlations with chemical structure. Amsterdam: Elsevier; 1972.
34. Qiu Z, Ikehara T, Nishi T. Miscibility and crystallization in crystalline/crystalline blends of poly(butylene succinate)/ poly(ethylene oxide). Polymer. 2003;44:2799–806.
35. Ziska JJ, Barlow JW, Paul DR. Miscibility in PVC-polyester blend. Polymer. 1981;22:918–23.
36. Avrami MJ. Kinetics of phase change. I: General theory. J Chem Phys. 1939;7:1103–12.
37. Avrami MJ. Kinetics of phase change. II Transformation-time relations for random distribution of nuclei. J Chem Phys. 1940; 8:212–24.
38. Avrami MJ. Granulation, phase change, and microstructure kinetics of phase change. III. J Chem Phys. 1941;9:177–84.
39. Castillo RV, Müller AJ, Raquez JM, Dubois P. Crystallization kinetics and morphology of biodegradable double crystalline PLLA-*b*-PCL diblock copolymers. Macromolecules. 2010;43: 4149–60.
40. Michell RM, Müller AJ, Deshayes G, Dubois P. Effect of sequence distribution on the isothermal crystallization kinetics and successive self-nucleation and annealing (SSA) behavior of poly(ε-caprolactone-*co*-ε-caprolactam) copolymers. Eur Polym J. 2010;46:1334–44.
41. Hamley IW, Castelletto V, Castillo RV, Müller AJ, Martin CM, Pollet E, Dubois P. Crystallization in poly(L-lactide)-*b*-poly (ε-caprolactone) double crystalline diblock copolymers: a study using X-ray scattering, differential scanning calorimetry, and polarized optical microscopy. Macromolecules. 2005;38: 463–72.
42. Achilias DS, Papageorgiou GZ, Karayannidis GP. Isothermal and nonisothermal crystallization kinetics of poly(propylene terephthalate). J Polym Sci B. 2004;42:3775–96.
43. Supaphol P. Application of the Avrami, Tobin, Malkin, and Urbanovici–Segal macrokinetic models to isothermal crystallization of syndiotactic polypropylene. Thermochim Acta. 2001;370: 37–48.
44. Dangseeyun N, Shrimoaon P, Supaphol P, Nithitanakul M. Isothermal melt-crystallization and melting behavior for three linear aromatic polyesters. Thermochim Acta. 2004;409:63–77.
45. Papageorgiou GZ, Bikiaris DN, Achilias DS. Effect of molecular weight on the cold-crystallization of biodegradable poly(ethylene succinate). Thermochim Acta. 2007;457:41–54.
46. Hoffman JD, Miller RL. Kinetic of crystallization from the melt and chain folding in polyethylene fractions revisited: theory and experiment. Polymer. 1997;38:3151–212.

47. Chan TW, Isayev AI. Quiescent polymer crystallization: modeling and measurements. Polym Eng Sci. 1994;34:461–71.
48. Papageorgiou GZ, Achilias DS, Bikiaris DN, Karayannidis GP. Crystallization kinetics and nucleation activity of filler in Polypropylene/surface-treated SiO_2 nanocomposites. Thermochim Acta. 2005;427:117–28.
49. Papageorgiou GZ, Achilias DS, Karayannidis GP. Estimation of thermal transitions in poly(ethylene naphthalate): experiments and modeling using isoconversional methods. Polymer. 2010;51:2565–75.
50. Sorrentino L, Iannace S, Di Maio E, Acierno D. Isothermal crystallization kinetics of chain-extended PET. J Polym Sci B. 2005;43:1966–72.
51. Papageorgiou GZ, Achilias DS, Bikiaris DN. Crystallization kinetics and melting behaviour of the novel biodegradable polyesters poly(propylene azelate) and poly(propylene sebacate). Macromol Chem Phys. 2009;210:90–107.
52. Immergut EH, Grulke EA, Abe A, Bloch DR. In: Brandrup J, editor. Polymer handbook. 4th ed. New York: Wiley; 1999.
53. Thomas DG, Stavely LAK. A study of the supercooling of drops of some molecular liquids. J Chem Soc. 1952;4569–77.